ELSEVIER

Sensors and Actuators 80 (2000) 132–137

SENSORS AND ACTUATORS A PHYSICAL

www.elsevier.nl/locate/sna

Prototype microrobots for micro-positioning and micro-unmanned vehicles

Paul E. Kladitis *, Victor M. Bright [1]

NSF Center for Advanced Manufacturing and Packaging of Microwave, Optical, and Digital Electronics (CAMPMODE), Department of Mechanical Engineering, University of Colorado at Boulder, Boulder, CO 80309-0427, USA

Received 15 April 1999; accepted 19 July 1999

Abstract

The design and performance of two prototype microrobots are presented in this paper. The microrobots were implemented by surface micromachining arrays of 270 μm long, polycrystalline silicon legs across the surface of a silicon chip. The method of motion of the microrobots is designed to mimic the way six-legged insects walk. One microrobot leg design has two degrees-of-freedom motion, and the other leg design has one degree-of-freedom motion. Both microrobot designs are able to transport objects across their bellies while lying on their backs. The microrobot with one degree-of-freedom motion is able to support several times its own weight, making available the option to carry an autonomous power supply (such as a solar cell), microprocessor, control circuitry, test equipment, and sensing or surveillance devices. Results of the self-assembly of the microrobot legs using the surface tension of molten indium are also presented.

Keywords: Microrobot; Electro-thermal actuator; Self-assembly; Solder; Insects

1. Introduction

The realization of the microrobot, presented herein, is a new and revolutionary tool useful for a variety of applications. Examples include micro-unmanned-surveillance vehicles and micro-weapons for military applications; small machines that help build smaller machines and small-quarters inspectors for industrial applications; and micro-surgeons for medical applications [1–3].

Several microrobot schemes, miniature robot designs, and microrobot components have been developed [4–9]. Some implementations have revealed important design considerations, for example, Teshigahara et al. [10] have determined that wheels are not a suitable method of propulsion for micrometer sized vehicles.

The method of motion for the robots in this research is modeled after the optimum designs already existing in nature. Mimicking nature is not a new concept in the field of Micro-Electro-Mechanical-Systems (MEMS). For example, Suzuki et al. [11,12] and Shimoyama et al. [6] replicate insect exoskeletons and insect wing muscle motion, and Ataka et al. [13] duplicate ciliary motion to transport objects across a chip.

This paper presents two microrobots designed to walk on a flat surface. The paper will discuss the method of motion and microrobot layout, the microrobot leg designs, and experimental performance of each microrobot. The microrobots in this research were fabricated using a commercially available silicon surface micromachining process: the Multi-User MEMS Process (MUMPs) by MCNC [14].

2. Method of motion and microrobot layout

The method of motion of both microrobots is designed to mimic the way six legged insects walk. In this method,

* Corresponding author. Tel.: +1-303-735-1734; fax: +1-303-492-3498; E-mail: kladitis@colorado.edu

[1] E-mail: victor.bright@colorado.edu

0924-4247/00/$ - see front matter
PII: S0924-4247(99)00258-7

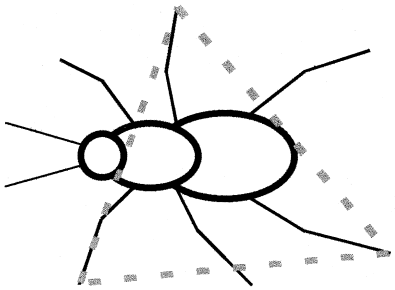

Fig. 1. Schematic of a six legged insect with three legs arranged in a tripod.

three legs, positioned like a tripod, are in contact with the walking surface at any one time. To copy this motion, the microrobots use large arrays of legs, electrically wired into six groups, to effectively act as six legs. Fig. 1 is a top view of a six-legged insect with three legs positioned in a tripod.

Fig. 2 shows a simplified wiring diagram used for both microrobots. Each leg of the microrobot is electrically powered. All the legs are grounded through the substrate. The six groups of legs are divided into two larger groups, where one group is powered with a signal through ''line A'', and the other group is powered through ''line B'' with a different signal, as shown in Fig. 2.

Power is applied to the microrobot through the three bondpads on the chip. Fig. 3 shows a scanning electron micrograph (SEM) of a belly-up view of a microrobot.

3. Microrobot leg designs

The wiring scheme and arrangement of leg groups are the same for both microrobot designs. The microrobots differ in leg design, size of the chip body, and the total number of legs. In both designs, the total number of legs is evenly divided into six groups.

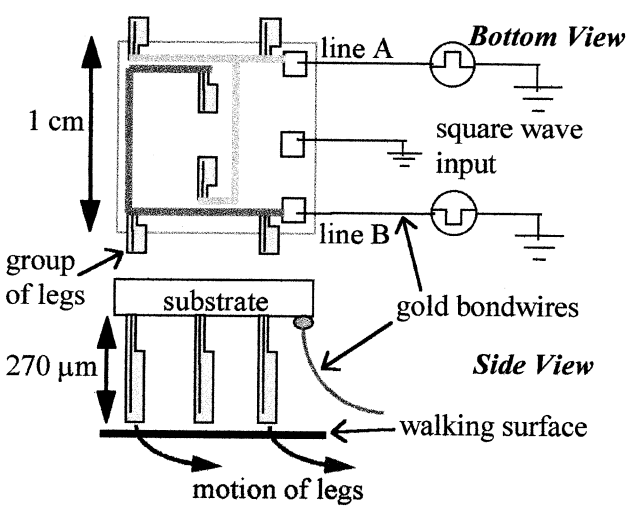

Fig. 2. Simplified wiring diagram for the microrobots showing a bottom or belly-up view and a side view.

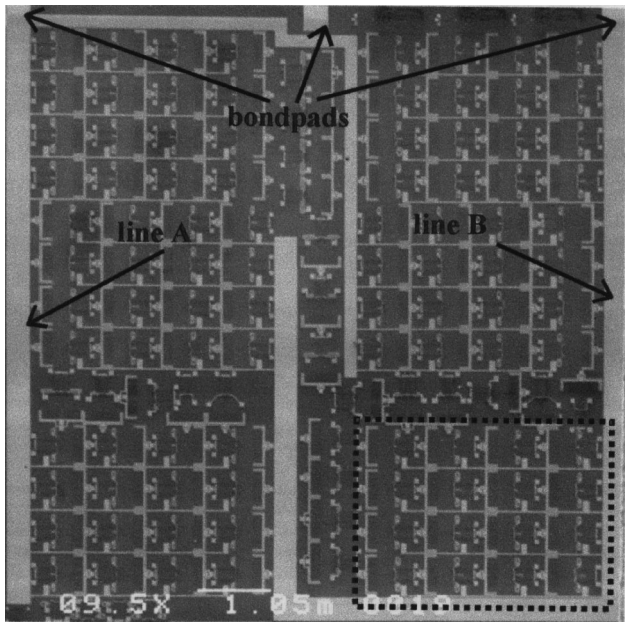

Fig. 3. SEM of a belly-up view of a microrobot. One of the six groups of legs is outlined by a dotted box.

3.1. Two degrees-of-freedom microrobot leg design

The two degrees-of-freedom microrobot design consists of a 1 cm × 1 cm × 0.5 mm silicon chip body with an array of 96 legs arranged into six groups of sixteen legs. Each leg is an electro-thermal actuator. An electro-thermal actuator takes advantage of the thermal expansion of polycrystalline silicon (polysilicon) when supplied by electric current [15]. The mass of this microrobot is 127.5 mg.

The 270 μm long by 18.5 μm wide by 2.0 μm thick legs are fabricated on one side of the chip using a polysilicon surface micromachining process. The legs are manually erected or assembled to a normal position with respect to the chip's surface and locked into place using microma-

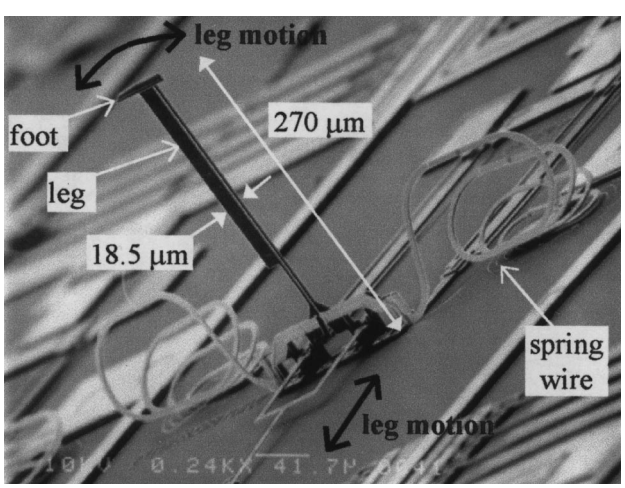

Fig. 4. SEM of an assembled microrobot leg with two degrees-of-freedom motion.

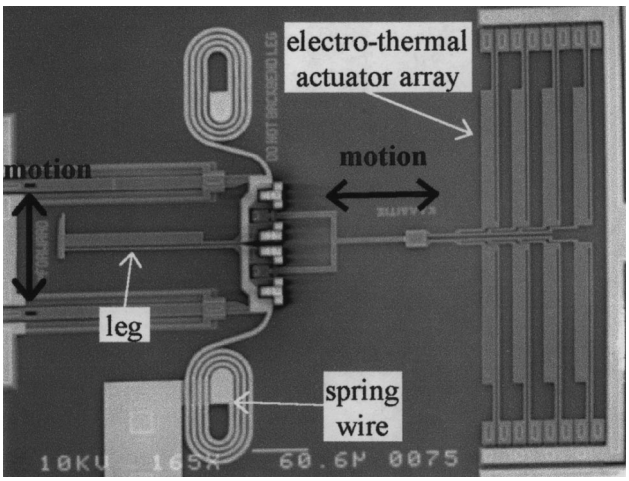

Fig. 5. SEM of an unassembled microrobot leg with two degrees-of-freedom motion.

nipulator probes. Electrical power is provided to each leg by two, gold covered, polysilicon connections called ‘‘ spring wires’’. The spring wires provide flexible and low resistance electrical connections from the leg to gold and polysilicon interconnects anchored to the substrate.

Fig. 4 shows an assembled microrobot leg. Fig. 5 shows an unassembled microrobot leg. The leg itself provides motion in the forward direction, and the electro-thermal actuator array, that can be seen in Fig. 5, provides motion in a sideways direction. Fig. 6 shows a portion of the microrobot (belly up) with several legs in view.

3.2. One degree-of-freedom microrobot leg design

The second microrobot design consists of a $5 \times 5 \times 0.5$ mm silicon chip body with an array of 90 electro-thermal actuators serving as legs. The legs are also fabricated using a polysilicon surface micromachining process, and have the same dimensions, as described for the two degrees-of-freedom case with the exception of being 3.5 μm thick.

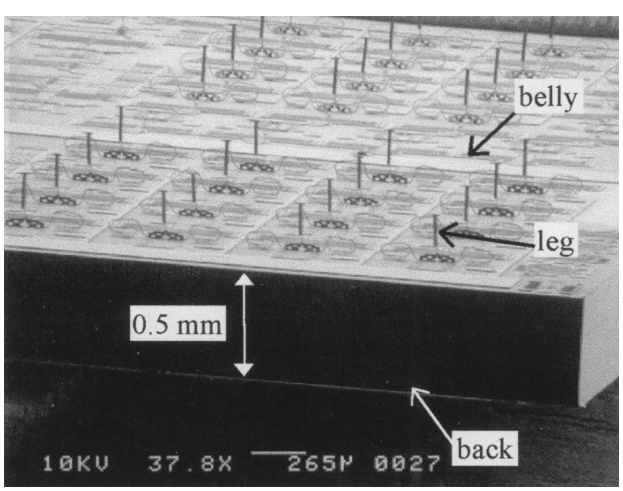

Fig. 6. A portion of the microrobot (belly up) with several legs in view.

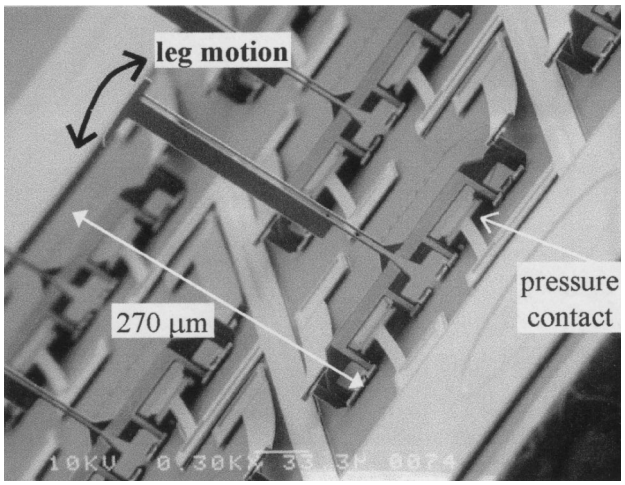

Fig. 7. SEM of a single one degree-of-freedom leg.

The mass of this microrobot design is 32 mg. The legs are manually erected to a normal position, with respect to the chip’s surface, using micromanipulator probes. Electrical power is provided to each leg by two polysilicon pressure contacts located at the base of each leg. Fig. 7 shows a SEM of one leg.

4. Experimental performance

4.1. Two degrees-of-freedom microrobot leg design

While positioned on its back (belly up), the two degrees-of-freedom microrobot legs were able to transport a 3.06 mg piece of kapton film ($9.25 \times 9 \times 0.023$ mm thick) across the microrobot belly. While carrying the piece of kapton film, the legs moved with a maximum step size of

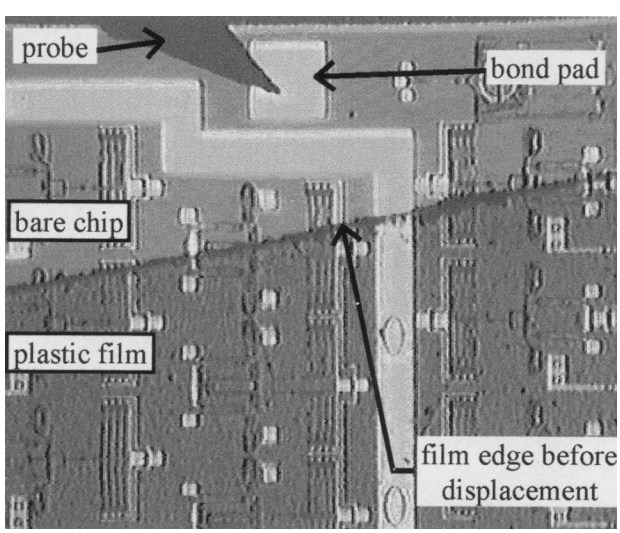

Fig. 8. Captured video image of a plastic film over the microrobot’s belly before being transported. Note the probe is supplying power to the microrobot through the bondpad.

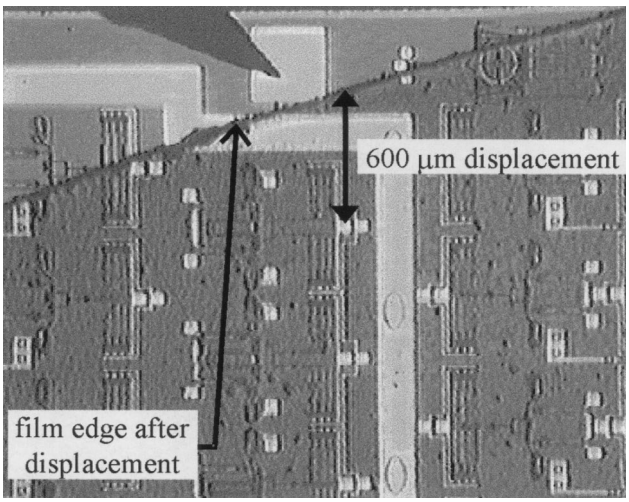

Fig. 9. Captured video image of a plastic film over the microrobot's belly after being transported.

3.75 μm at 453 μm/min powered by a 0–5 V square wave input with a 50% duty cycle and frequency of 2 Hz. Thus, this experiment demonstrated a voltage-controlled micropositioner. The signal applied to ''line A'' is 180° out of phase with the signal to ''line B''. Figs. 8 and 9 are a series of video images showing the plastic film before and after transport over the microrobot's belly. In Figs. 8 and 9, the belly of the robot can be seen through the plastic film while being transported by the microrobot's feet. The maximum DC power that may be supplied to this design, before the electro-thermal actuator polysilicon legs melt, was measured as being 10 V × 287 mA = 2.87 W.

Both microrobot designs were also tested by placing them, legs down, on a walking surface while being connected to a remote power supply. The microrobot was connected to the remote power supply using three 25 μm diameter and 5 in. long gold bonding wires. However, the gold wires turned out to be too massive and stiff to permit movement or even allow all the microrobot feet to touch the walking surface. Future designs will carry an autonomous power supply. The future designs will be optimized for power consumption in order to be powered by solar cells or a thin film battery.

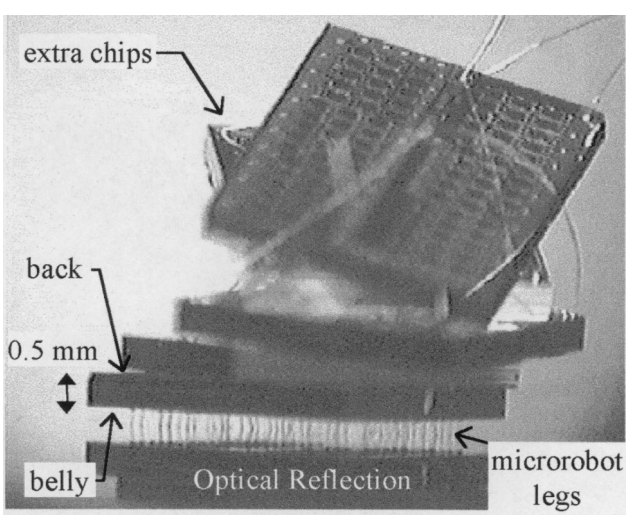

Fig. 10. Captured video image of the microrobot supporting four silicon chips plus gold bonding wire. The microrobot is standing on a silicon wafer.

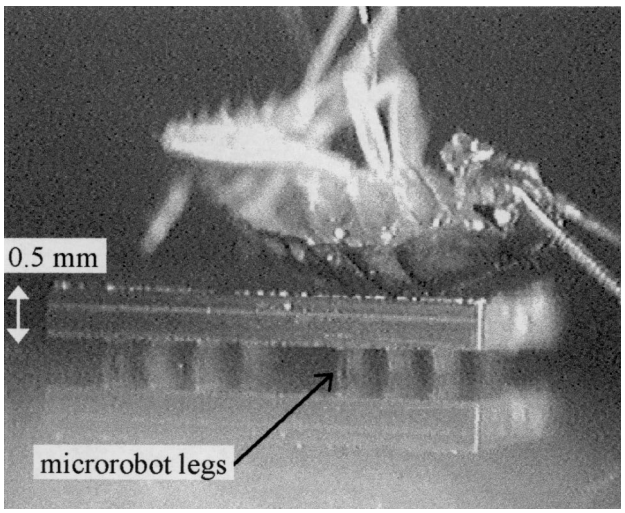

Fig. 11. Video image of the microrobot supporting an insect.

4.2. One degree-of-freedom microrobot leg design

While positioned on its back (belly up), the one degree-of-freedom microrobot was able to transport a chip of equal size (32 mg) across its belly while being powered by a square wave input. The signal applied to ''line A'' was 180° out of phase with the signal applied to ''line B''. The maximum DC power that may be supplied to this design, before the electro-thermal actuator polysilicon legs melt, was measured as being 8 V × 74 mA = 592 mW.

Standing on its legs, on a silicon wafer, this microrobot can support several times its own weight. Fig. 10 shows a captured video image of the microrobot supporting four silicon chips plus gold bonding wire. The microrobot legs collapsed after the loading of a fifth chip. Fig. 11 shows the microrobot supporting a cockroach. The chips (32 mg each) and the cockroach (unknown weight) were lowered onto the microrobot's back using tweezers.

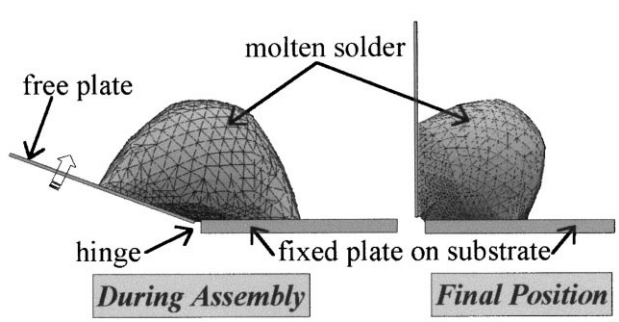

Fig. 12. Illustration of solder self-assembly of a hinged plate.

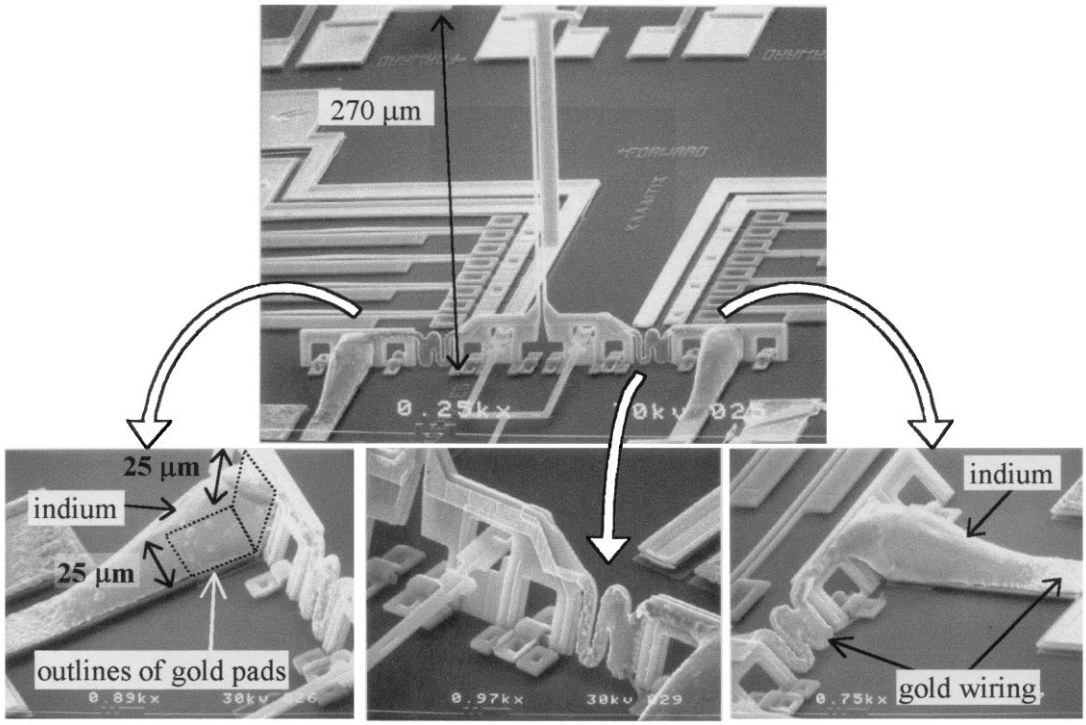

Fig. 13. SEM of a single solder self-assembled microrobot leg showing close views of the left and right indium solder joints and the electro-mechanical linkage isolating the right solder joint from the leg.

4.3. Towards self-assembly of microrobot legs

As stated previously, all of the microrobot legs were manually assembled using micromanipulator probes. The average time for assembly per microrobot was typically 3 h. Damaging the legs during the assembly was a common problem. Current research is directed on massively parallel solder assembly [16–20] of the microrobot legs to make the microrobots commercially manufacturable.

Solder assembly of MEMS involves the use of the surface tension of molten solder as the assembly mechanism. The solder assembly method uses polysilicon plates hinged to the substrate with specific areas metallized as solder wettable pads. Once the solder is in place, it is heated to its melting point, and the force, produced by the natural tendency of liquids to minimize their surface energy, pulls the free plate away from the silicon substrate, as illustrated in Fig. 12. Using solder, hundreds or thousands of precision alignments can be accomplished with a single batch reflow process.

Current results of using surface tension to assemble microrobot legs are shown in Fig. 13. The equivalent of a sphere of indium with diameter of 37 μm was deposited on each set of 25×25 μm gold pads for the microrobot leg shown in Fig. 13. The outline of the location of the gold pads is also shown in Fig. 13.

The pure indium was evaporated, using a BAL-TEC MED 020 Coating System, and patterned on the chip using a thick photoresist (AZ P4620) metal lift-off process before sacrificial oxide etch of the surface micromachined microrobot legs. The chip was then heated to the melting point of the indium (160°C), where the surface tension of the molten indium lifted the legs into place as shown in Fig. 13. The microrobot leg, shown in Fig. 13, is one of five legs fabricated on a 2×2 mm test chip.

This new microrobot leg design combines the sturdiness of the 3.5 μm thick one degree-of-freedom leg design with two degrees-of-freedom motion. The indium solder joints serve as low resistance electrical connections and mechanically rigid supports for the legs, making the robot leg design robust. A curved spring-like electro-mechanical linkage isolates the mechanically rigid solder joints from the leg, permitting the two degrees-of-freedom motion.

5. Conclusions

This paper presented the design and experimental results for two microrobot prototypes. The two degrees-of-freedom microrobot design demonstrated transportation of a piece of plastic film in a single direction. However, the legs posses two degrees-of-freedom motion in the plane of the chip. Depending on the wiring and synchronization of leg movements, the robot could transport or rotate an object in any direction within the plane of the chip, thus realizing a micropositioner. The one degree-of-freedom microrobot design demonstrated transportation of a chip of the same size and was able to support up to four chips.

Providing an autonomous power supply or a power supply that would not impede movement of both microrobots was a challenge in this research. However, the one degree-of-freedom microrobot design should easily be able to carry an autonomous power supply (such as a solar cell), microprocessor, control circuitry, test equipment and sensing or surveillance devices, thus realizing a micro-unmanned vehicle.

The ability of being able to assemble the microrobot legs using the surface tension of solder makes the mass production of this microrobot a reality by simply adding a solder deposition step and reflow step to a MEMS fabrication process.

Acknowledgements

This effort was sponsored in part by the Department of Defense (MDA904-97-C-0320) and Defense Advanced Research Projects Agency (DARPA) and Air Force Research Laboratory, Air Force Materiel Command, USAF, under agreement number F30602-98-1-0219.

References

[1] P. Dario, R. Valleggi, M.C. Carrozza, M.C. Montesi, M. Cocco, Microactuators for microrobots: a critical survey, Journal of Micromechanics and Microengineering 2 (3) (1992) 141–157.

[2] S. Johansson, Micromanipulation for micro- and nano-manufacturing, Proceedings of the INRIA/IEEE Symposium on Emerging Technologies and Factory Automation, Vol. 3, 1995, pp. 3–8.

[3] M. Flynn, L. Tavro, S. Bart, R. Brooks, D. Ehrlich, K. Udayakumar, L. Cross, Piezoelectric micromotors for microrobots, IEEE/ASME Journal of Microelectromechanical Systems 1 (1) (1992) 44–51.

[4] T. Fukada, A. Kawamoto, F. Arai, H. Matsuura, Micro mobile robot in fluid (1st report, mechanism and swimming experiment of micro mobile robot in water), Transactions of the Japan Society of Mechanical Engineers, Part C 60 (569) (1994) 204–210.

[5] C. Liu, T. Tsao, Y. Tai, W. Liu, P. Will, C. Ho, Micromachined permalloy magnetic actuator array for micro robotics assembly systems, Proceedings of the International Conference on Solid-State Sensors and Actuators, Eurosensors IX, Vol. 1, 1995, pp. 328–331.

[6] I. Shimoyama, Y. Kubo, T. Kaneda, H. Miura, Simple microflight mechanism on silicon wafer, Proceedings of the IEEE MEMS Workshop, 1994, pp. 148–152.

[7] T. Yasuda, I. Shimoyama, H. Miura, Microrobot actuated by a vibration energy field, Sensors and Actuators, A: Physical 43 (1) (1994) 366–370.

[8] R. Yeh, E. Kruglick, K. Pister, Towards an articulated silicon microrobot, Proceedings of ASME Dynamic Systems and Control, Vol. 2, 1994, pp. 747–754.

[9] R. Yeh, E.J.J. Kruglick, K.S.J. Pister, Surface-micromachined components for articulated microrobots, IEEE/ASME Journal of Microelectromechanical Systems 5 (1) (1996) 10–17.

[10] A. Teshigahara, M. Watanabe, N. Kawahara, Y. Ohtsuka, T. Hattori, Performance of a 7-mm microfabricated car, IEEE/ASME Journal of Microelectromechanical Systems 4 (2) (1995) 76–80.

[11] K. Suzuki, I. Shimoyama, H. Miura, Insect-model based microrobot with elastic hinges, IEEE/ASME Journal of Microelectromechanical Systems 3 (1) (1994) 4–9.

[12] K. Suzuki, I. Shimoyama, H. Miura, Y. Ezura, Creation of an insect based microrobot with an external skeleton and elastic joints, Proceedings of the IEEE MEMS Workshop, 1992, pp. 190–195.

[13] M. Ataka, S. Omofsks, N. Takeshima, H. Fujita, Fabrication and operation of polyimide bimorph actuators for a ciliary motion, IEEE/ASME Journal of Microelectromechanical Systems 2 (4) (1993) 146–150.

[14] D. Koester, R. Mahadevan, K. Markus, SmartMUMPs design handbook including MUMPs introduction and design rules, rev. 4, DARPA project (DABT 63-93-C-0051) of MEMS Technology Applications Center MCNC, 3021 Cornwallis Road, Research Triangle Park, NC 27709, 1996.

[15] J.H. Comtois, V.M. Bright, Applications for surface micromachined polysilicon thermal actuators and arrays, Sensors and Actuators, A: Physical 58 (1997) 19–25.

[16] R.R.A. Syms, Equilibrium of hinged and hingeless structures rotated using surface tension forces, Journal of Microelectromechanical Systems 4 (4) (1995) 177–184.

[17] P.W. Green, R.R.A. Syms, E.M. Yeatman, Demonstration of three-dimensional microstructure self-assembly, Journal of Microelectromechanical Systems 4 (4) (1995) 170–176.

[18] K. Harsh, R. Irwin, Y.C. Lee, Solder self assembly for MEMS, Proceedings of the 44th International Instrumentation Symposium, Reno, NV, May 1998, pp. 249–255.

[19] K. Harsh, Y.C. Lee, Modeling for solder self-assembled MEMS, Proceedings of SPIE 3289 (1998) 177–184.

[20] P.E. Kladitis, V.M. Bright, K.F. Harsh, Y.C. Lee, Prototype microrobots for micro positioning in a manufacturing process and micro unmanned vehicles, The 12th IEEE International Conference on MicroElectroMechanical Systems — MEMS '99, Orlando, FL, 17–21 January 1999, pp. 570–575.

Paul Kladitis is currently working on a PhD in Mechanical Engineering at the University of Colorado at Boulder. He received his BS in Electrical Engineering at Wright State University in Dayton, OH in 1996 and his MS in Electrical Engineering at the Air Force Institute of Technology in Dayton, OH in 1997.

Dr. Victor M. Bright is an Associate Professor of Mechanical Engineering and the Director of the MEMS R&D Laboratory, University of Colorado at Boulder. Prior to joining the University, he was an Associate Professor and the Director of Microelectronics Research Laboratory in the Department of Electrical and Computer Engineering, Air Force Institute of Technology, Wright–Patterson Air Force Base, OH (6/92–12/97). Prof. Bright's research includes MEMS, silicon micromachining, microsensors, microactuators, MEMS self-assembly, MEMS packaging, opto-electronics, and semiconductor device physics. Dr. Bright received the following awards in the area of MEMS: Best Paper of the MCM'98 — International Conference and Exhibition on Multichip Modules and High Density Packaging, 1998; R.F. Bunshah Best Paper Award at the 1996 International. Conference on Metallurgical Coatings and Thin Films. Dr. Bright has authored and co-authored more than 70 papers in the areas of MEMS. He is a member of IEEE, ASME, and SPIE. He serves on the Executive Committee for ASME MEMS Sub-division.